Synthetic antenna functioning as light harvester in the whole visible region for enhanced hybrid photosynthetic reaction centers.

Omar Hassan Omar[†], Simona la Gatta[§], Rocco Roberto Tangorra[§,#], Francesco Milano[‡], Roberta Ragni[§], Alessandra Operamolla[§], Roberto Argazzi[|], Claudio Chiorboli[|], Angela Agostiano[§,‡], Massimo Trotta[‡,*] and Gianluca M. Farinola[§,*]

† Istituto di Chimica dei Composti Organometallici, Consiglio Nazionale delle Ricerche – Bari, Italy

§ Dipartimento di Chimica, Università degli Studi di Bari "Aldo Moro" - Bari, Italy

‡ CNR-IPCF Istituto per i Processi Chimico Fisici, Consiglio Nazionale delle Ricerche – Bari, Italy

| Istituto di Sintesi Organica e Fotoreattività, Consiglio Nazionale delle Ricerche – Ferrara, Italy

Supporting Information Placeholder

ABSTRACT: The photosynthetic Reaction Center (RC) from the *Rhodobacter sphaeroides* bacterium has been covalently bioconjugated with a NIR-emitting fluorophore (AE_{800}) whose synthesis was specifically tailored to act as artificial antenna harvesting light in the entire visible region. AE_{800} has a broad absorption spectrum with peaks centred in the absorption gaps of the RC and its emission overlaps the most intense RC absorption bands, ensuring a consistent increase of the protein optical cross-section. The covalent hybrid AE_{800}-RC is stable and fully functional. The energy collected by the artificial antenna is transferred to the protein via FRET mechanism, and the hybrid system outperforms by a noteworthy 30% the overall photochemical activity of the native protein under the entire range of visible light. This improvement in the optical characteristic of the photoenzyme demonstrates the effectiveness of the bioconjugation approach as a suitable route to new biohybrid materials for energy conversion, photocatalysis and biosensing.

INTRODUCTION

In photosynthesis solar radiation is converted in metabolic energy by means of the photosynthetic apparatus, a multi-protein array designed by evolution to absorb light and convert it into high energy molecules. Plants, algae, cyanobacteria and photosynthetic bacteria all share the common basic protein architecture formed by a photochemical core, where the actual energy conversion takes place, the reaction center (RC), in intimate contact with a light harvesting complex (LHC) devoted to collect light and to transfer the collected energy to the photoconversion unit. The photoconversion process, functioning with an efficiency yet unmatched by any artificial system[1,2] eventually fuels metabolic activities of the organisms.

Anoxygenic photosynthetic bacteria are believed to be the ancestors of all photosynthetic organisms[3] and nowadays occupy only a very small and often disregarded ecological niche. However, they have risen to great interest in the scientific community as their relatively simple photosynthetic apparatus has been used for understanding the molecular mechanism of light conversion and as a model for the more complex photosynthetic apparatus of oxygen evolving organisms. The combination of efficient photoconversion ability, relative simplicity and wealth of structural and dynamic available information makes the reaction center of the purple bacterium *Rhodobacter* (*R.*) *sphaeroides* a handy protein for materials scientists interested in photoactive biomolecules for energy conversion[4,5], photocatalysis[6,7] and biosensing[8] applications.

The RC is an integral membrane protein which can be easily isolated and purified and used for applicative purposes, with the sole attention of maintaining its hydrophobic portion shielded from water by mean of suitable surfactants molecules[9]. The protein is composed of three subunits (M, L and H, Figure 1) encaging nine non covalently bound cofactors, *i.e.* four bacteriochlorophylls (two forming a dimer D facing the periplasmic side and two in monomeric form $BChl_A$ and $BChl_B$), two bacteriopheophytins BPh_A and BPh_B, two ubiquinone-10 molecules Q_A and Q_B, and one non-heme Fe^{2+} ion. The cofactors are arranged in two quasi-symmetric branches indicated as A and B as shown in Figure 1.

The cofactors are directly responsible for the light induced electron transfer cascade process: upon photon absorption, the primary electron donor D is excited and rapidly transfers one electron, within nanoseconds, to the primary ubiquinone (Q_A). The electron eventually reaches in 100 microseconds the secondary (Q_B) ubiquinone acceptor. In presence of the physiological electron donor, the reduced form of cytochrome c_2, and a pool of quinone, the protein undergoes to a photocycle that ultimately rises the pH in the cytoplasm of the bacterium.

Dislodged from the cell and deprived of the physiological exogenous electron donors, the isolated protein, under irradiation, produces the long living (1-3 sec) electron-hole couple $D^+Q_B^-$. In isolated form the RC can be regarded as an efficient molecular photoconverter amenable for many potential applications[10].

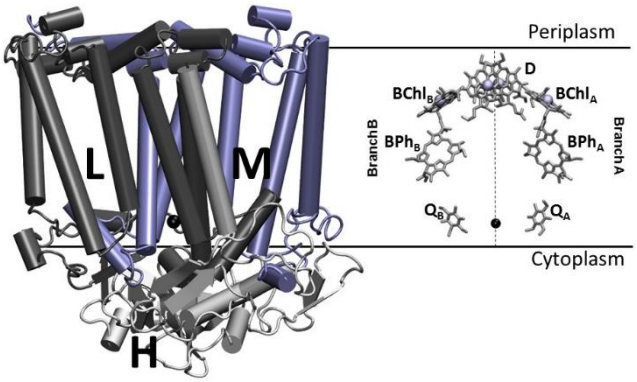

Figure 1. Structure of the protein scaffolding (left) and spatial organization of the cofactors (right) within the reaction center from the carotenoidless strain R26 of the photosynthetic bacterium *R. sphaeroides*. Letters A and B indicate the two branches of the cofactors. The hydrophobic chains of the cofactors are not shown. The non-heme iron Fe^{2+} is shown as a sphere. Adapted from Tangorra *et al.*[11] with permission from the European Society for Photobiology, the European Photochemistry Association, and The Royal Society of Chemistry.

Although the RC conversion efficiency of absorbed photons into electron-hole pairs is close to unity, the direct light capture of the bare protein is intense in the near infrared (NIR) region and limited in the visible region, where solar irradiance is maximum. Therefore, extending the RC visible absorption cross-section to the photosynthetic active region (PAR) is highly desirable to employ this protein as efficient hybrid photoconverter. Nature has indeed selected the same strategy by surrounding the RC with two antenna proteins (LH1 and LH2) which efficiently collect solar light and funnel it to the RC. It is possible to isolate and purify[12] a functional RC:LH2 complex from *R. sphaeroides* in which the central RC and the LH2 are closely connected. Nevertheless, the absence of covalent binding between antenna and RC makes the system delicate and susceptible to degradation.

To extend the visible absorption cross-section of isolated RC, various strategies have been recently developed based on the RC integration with suitable organic or inorganic light harvesting components[13]. Among them, the covalent conjugation of specific RC aminoacid residues with tailored unhindered organic dyes was proven to be very profitable also in view of protein activity preservation. In a previous work we covalently bound to the amino groups of RC lysine residues[5] a tailored aryleneethynylene (AE) dye characterized by high absorptivity, good fluorescence yield (23%) in aqueous solution, and a consistent Stokes shift (150 nm). The molecule was designed to absorb at 450 nm, where the protein has a flat absorption profile, and to emit at 600 nm in correspondence of one of the protein absorption peaks. When bioconjugated to the RC, AE_{600} proved to be very effective as antenna: the hybrid outperformed the native protein by a factor of five in the yield of electron-hole couple formation and the enzymatic activity resulted increased by a factor of three. However, this impressive improvements were limited to the maximum absorption wavelength of AE_{600} at 450 nm.[5] The result was reproduced in a number of recently published articles in which the role of the antenna is played by commercial dyes such as fluorescein isothiocyanate (FITC)[14] bioconjugated to RC from strain *R. sphaeroides* R26 and three different commercial dyes[15] bioconjugated to a triple mutant of the strain *R. sphaeroides* 2.4.1. Alexa Fluor were also used as antenna molecules in combination with a 3-arm-DNA fragment.[16] In all cases, the organic dye functions as antenna and the hybrid system outperforms the native protein activity. The ability of organic antenna to enhance and improve energy transfer has also been proven for the photosynthetic bacterial light-harvesting complex LH2 from *Rhodopseudomonas acidophila* strain 10050.[17] Recently, the artificial antenna concept was extended also to the photosystem I (PSI) extracted from the thermophilic cyanobacterium *Thermosynechococcus elongatus*.[18]

All the artificial antennas reported so far have drawbacks: limited photostability in aqueous buffered solutions (Alexa Fluor dyes and FITC)[19], narrow absorption bands, light emission in correspondence of minor absorption peaks of the protein (AE_{600} and FITC) or small Stokes shift (ranging from 15 to 50 nm in the Near Infrared Region (NIR) for the Alexa Fluor dyes) giving rise to auto-absorption phenomena. As a consequence, the ability of these dyes to work as antennas is limited to a small portion of the visible spectrum or require a consistent antenna-to-protein ratio.

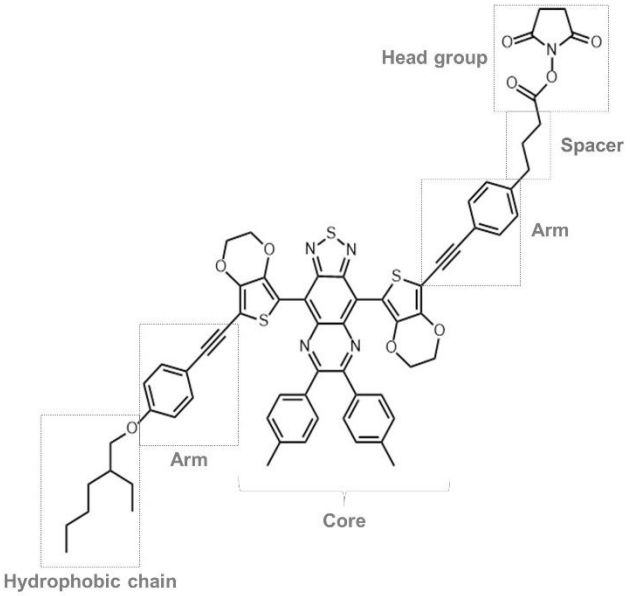

Figure 2. Chemical structure of AE_{800}. The different parts of the molecule have been identified by dotted squares.

In this article we present a molecule (AE_{800} in Figure 2) that, similarly to the physiological LHC, is able to harvest light in the visible region (400-700 nm, the PAR of plants and algae) and to emit in correspondence of the NIR intense absorption peaks of the RC protein. The organic biological hybrid obtained with this carefully designed molecule outperforms the photoconversion efficiency of the native protein by 30% under white light excitation, thus fully mimicking the function of the natural light harvesting complexes with a simple and robust molecule.

RESULTS AND DISCUSSION

Chemical design of AE_{800}

Efficient organic antennas for RC must be properly designed to (*a*) absorb solar radiation in the PAR region (400 – 700 nm); (*b*) possess a large Stokes shift to minimize self-absorption; (*c*) emit in correspondence of the most intense absorption peaks of the RC (700–900 nm); (*d*) possess a proper photoluminescence quantum yield in aqueous medium; (*e*) covalently bind the protein without jeopardizing the enzymatic activity and, (*f*) be sterically flexible to avoid cluttering RC in the interaction with the exogenous electron donor.

Scheme 1. Synthesis of AE_{800}.

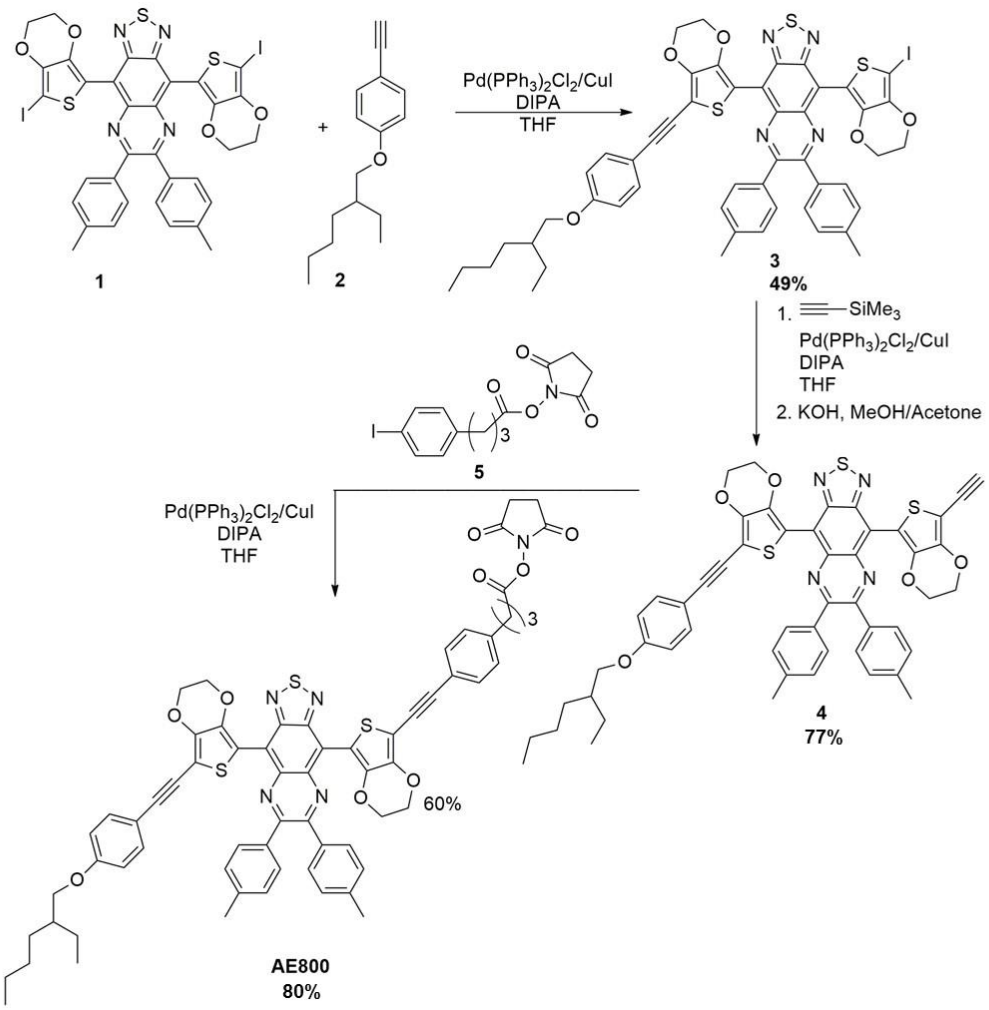

AE_{800} (Figure 2), similarly to our previously reported AE_{600} antenna molecule,[5] is specifically designed to fulfil the requirements. Its structure bears a peripheral succinimidyl ester group enabling selective bioconjugation to the lysines of RC. A *n*-propyl spacer is inserted between the anchoring moiety and the π-conjugated skeleton of the antenna to reduce its rigidity and sterical hindrance in correspondence of the enzyme surface. The π-conjugated backbone has been properly designed to fulfil the (*a*) and (*b*) spectroscopic requirements.

According to the literature, various structural motifs of NIR dyes are in principle eligible, including squaraines and cyanines. Squaraines, despite being highly efficient and stable NIR emitting molecules, have very low Stokes shift.[20] Cyanines exhibit highly intense NIR photoluminescence but they often suffer from low photostability in aqueous medium.[21,22] Porphyrins[23] can also be used but the insertion of suitable functional groups for selective anchoring to amminoacid RC residues may result in a very challenging task.

Organic conjugated molecules bearing an alternation of electron donor (D) and acceptor (A) units are well known low band gap molecules suitable as active materials for organic solar cells[24-28] or light emitting diodes.[29-31] In particular, a proper selection of D and A structures may lead to D-A-D molecules with light absorption in the visible range and emission in the NIR region. In our case, the core moiety **(**Figure 2**,** Table **1**), bearing two ethylenedioxythiophenes (EDOT) and a thiadiazole quinoxaline (TQ), absorbs and emits light with good efficiency and large Stokes shift ($\lambda_{max\ abs}$: 570 nm, $\lambda_{max\ em}$: 710 nm).[32-35] We have hence designed a chemical structure resulting from the extension of the core with two peripheral phenyleneethynylene arms expected to both enhance PL efficiency and red-shift absorption and emission of AE_{800}. Polymers and small molecules with aryleneethynylene conjugated structure are stable and efficient emitting materials whose synthesis is compatible with the insertion of reactive groups suitable for their covalent conjugation to biomolecules.[36-42] To increase the hydrophobicity of the antenna, a 2-ethylhexyl chain was introduced, further ensuring the interactions with the tensioactive molecules surrounding the isolated RC.

Synthesis of AE_{800}

AE_{800} was synthesized according to Scheme 1. The synthetic pathway involves three palladium catalyzed Cassar-Heck-Sonogashira cross-coupling reactions which were carried out under the same experimental conditions, *i.e.* in dry THF solvent and in the presence of $Pd(PPh_3)_2Cl_2$, CuI and diisopropylamine as the catalyst, the co-catalyst and the base, respectively. The first cross-coupling process was performed between compounds **1** and **2,** yielding the aryl iodide **3** (49%). This product was then coupled with trimethylsilylacetylene and the resulting product was directly converted into **4** by desilylation reaction with KOH carried out in a mixture of methanol and acetone as the solvent. Finally, the cross coupling reaction of alkyne **4** with the aryl iodide **5** led to AE_{800} in 80% yield.

The synthetic pathway to the central D-A-D building block **1** (Scheme 2) involves the preliminary synthesis of the aryldibromide **7** by a double step synthetic procedure with a higher yield (92%) than literature.[43] The procedure is based on the nitration reaction of commercially available 4,7-dibromobenzo[1,2,5]thiadiazole, the reduction of the resulting dinitro derivative **6** with iron in acetic acid and the condensation of the diamino intermediate product with the 1,2-di-*p*-tolyl-ethane-1,2-dione. The preparation of the compounds **6**,[44] to the best of our knowledge, gave the highest yield reported in the literature (see comparison of nitration with the classical pair H_2SO_4/HNO_3 in supporting information).[45,46]

Then, the palladium catalyzed Suzuki-Miyaura cross-coupling reaction of **7** with the pinacol boronic ester **8**[47] in presence of S-phos as a ligand, yielded almost quantitatively the symmetric product **9** which was finally subjected to a double iodination reaction with *N*-iodosuccinimide to obtain **1** in 95% yield. The ester **8** was prepared in enhanced yield with respect to literature.[48]

Scheme 2. Synthesis of building block 1.

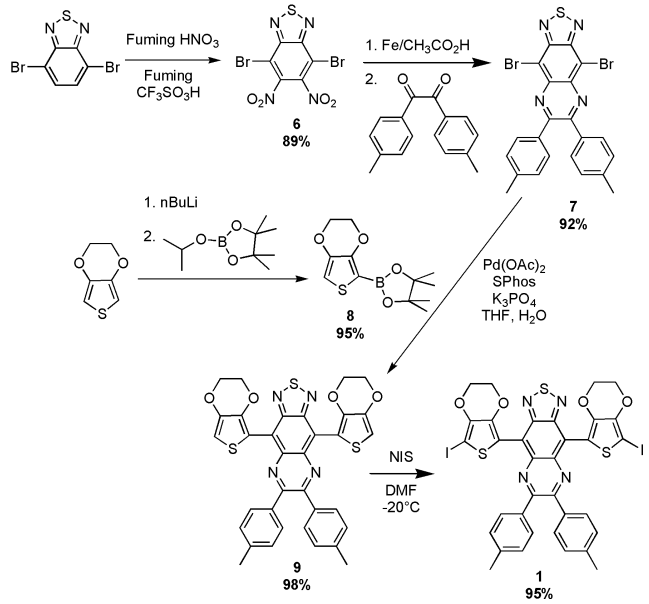

Alkyne **2**[49] was obtained in good yield by alkylation reaction of 4-iodophenol with 1-bromo-2-ethylhexane at room temperature in the presence of KOH and DMSO as the base and the solvent, respectively. Subsequent cross-coupling of the aryl iodide **10**[50] with trimethylsilylacetylene was performed under the same experimental conditions of previously described Sonogashira reactions in Scheme 1. The obtained product was directly subjected to desilylation reaction with KOH, yielding the alkyne **2** in 91% (desilylation reaction) or 83% (overall yield, starting from the aryl iodide **10**) (Scheme 3).

Scheme 3. Synthesis of building block 2.

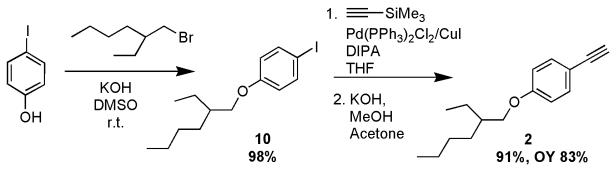

The aryl iodide **5** was prepared in 93% yield by activation reaction of the 4-(4-iodophenyl)butanoic acid with *N*-hydroxysuccinimide in the presence of 1-ethyl-3-(3-dimethylaminopropyl)carbodiimide in dry dichloromethane at 0 °C (Scheme 4).

Scheme 4. Synthesis of building block 5.

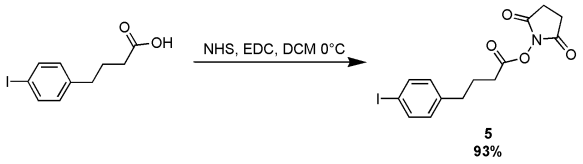

Spectroscopic characterization of AE_{800}

Owing to the extension of the π-conjugated backbone, AE800 absorption and emission maxima perfectly suited for our purpose. The photophysical properties of AE800 were also investigated in TX-100 aqueous buffer in which the bare RC membrane protein is kept stable, by a toroid of detergent molecules surrounding the hydrophobic surface of the protein. Data are summarized in

Table 1. Absorption and emission spectra of AE800 and its core moiety in chloroform are presented in supporting information (see Figure S2).

The decrease in the fluorescence quantum yield of AE_{800} compared to the core is expected since quantum yield systematically decreases when the emission shifts to the NIR region[32] as a result of the competition between radiative and non-radiative decay processes.[51]

The optical spectra of RC in the range 1100-250 nm were recorded using a UV-Vis-NIR Cary 5000 spectrophotometer (Agilent Technologies – USA) and contain several peaks associated to the electronic transition of the pigments and the protein scaffold.[52] In the Vis-NIR region the protein shows absorption maxima at 535, 600, 760, 802 and 865 nm, while AE_{800} has shoulder around 450 nm and a broad peak centered at 650 nm (Figure 3). The wavelengths 450 and 650 nm were selected to investigate the AE_{800} antenna effect using the 800 nm as reference wavelength.

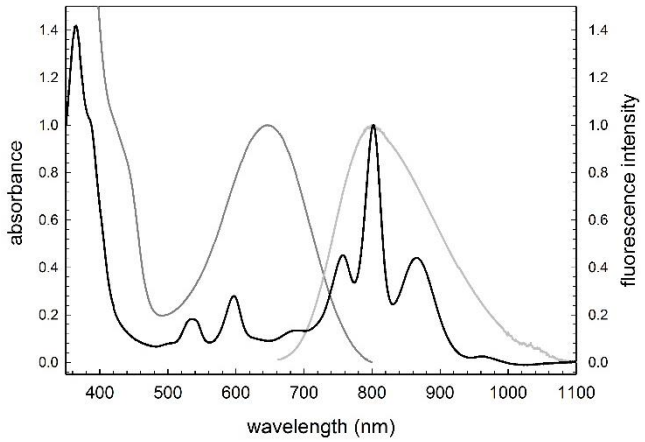

Figure 3. AE_{800} (98 μM) absorption and emission spectra, in dark and light grey, respectively compared to the RC (3.3 μM) absorption spectrum. Spectra are collected at pH 8.0 in $T_{20}E_1TX_3$ and $T_{20}E_1TX_{0.3}$ respectively.

Bioconjugation of AE_{800} to the RC

AE_{800} was covalently attached to the RC by condensation reaction of the succinimidyl ester moiety of AE_{800} with the amino groups of the lysine residues in RC, according to the procedure outlined in the experimental section [5,14,53]. The reaction is performed in a $T_{20}E_1TX_{0.3}$ buffer solution at pH 8. To obtain an adequate concentration of AE_{800}, its stock solution was prepared in $T_{20}E_1TX_3$ buffer (see Figure S1 in supporting information). The micelles solubilizing AE_{800} molecules convey it to the detergent toroid of the protein, driving them to react with the lysine residues located in this region. Nine lysines close to the detergent belt are also located in close proximity of the chlorin pigments, and represent the most

appropriate position for efficient energy transfer. The covalent binding of organic antenna molecules produces two bumps in the spectrum of the protein in correspondence of the main absorptions of the dye (Figure 4). From the relative contribution of AE_{800} and the RC in the optical spectrum of the hybrid obtained in several different preparations, an average number of 4.9±0.1 antenna molecules per protein is estimated. Adventitious binding between the fluorophore and the RC was ruled out in a control experiments performed using AE_{800} lacking the activating group NHS. Ionic chromatography of a mixture formed by the non-activated fluorophore and the protein shows that AE_{800} and RC emerge in distinctly separated peaks. Applying ionic chromatography to a solution containing the bioconjugated hybrid obtained using the activated fluorophore, the AE_{800}-RC elutes in a single peak at the same ionic strength of the sole protein. The data, including the average ratio AE_{800}-RC are shown in Figure S4 in the supporting information.

Based on crystallographic information[54] and on the AE_{800} chemical structure, it is possible to estimate the distances between the π-conjugated antenna backbone and the bacteriochlorophylls within the RC, which is found equal or lower than 48 Å. From Eq. 2, using the data summarized in

Table 1, a Förster critical radius R_0 = 60 Å of the hybrid AE_{800}-RC system can be calculated.[55] Since the AE_{800}/BChl distance is shorter than R_0 by at least 12 Å, it can be assumed that the antenna molecules transfer the harvested energy to the RC via FRET mechanism.

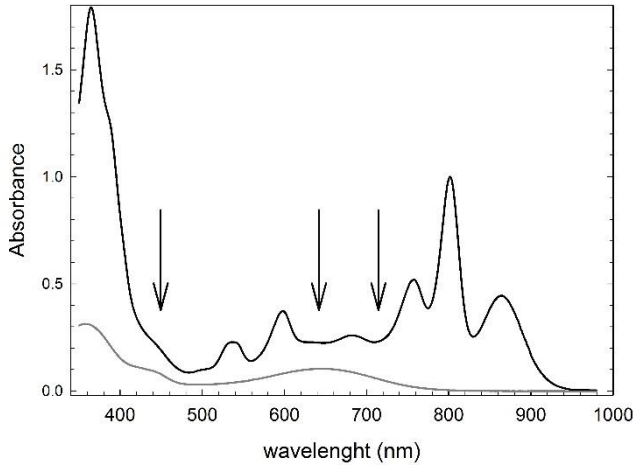

Figure 4. Absorption spectrum of the AE_{800}-RC hybrid in $T_{20}E_1TX_{0.3}$ (black [RC] = 1 μM) and of the sole AE_{800} in $T_{20}E_1TX_3$ (gray, [AE_{800}] = 10 μM). pH 8.0. Arrows indicate the wavelengths where the RC has small absorption and AE_{800} contributes the most to the AE_{800}-RC hybrid spectrum.

Energy Transfer Efficiency

The steady-state emission of AE_{800} and AE_{800}-RC hybrid in the range 700-1100 nm is shown in Figure 5 The maximum emission wavelength results unchanged, but the fluorescence intensity, corrected for the internal absorption, in the hybrid system is 38% of the fluorescence measured in the antenna. The noticeable AE_{800} emission quenching associated to the bioconjugation is consistent with energy transfer to RC pigments with an actual FRET efficiency of 62% calculated according to Equation 1.

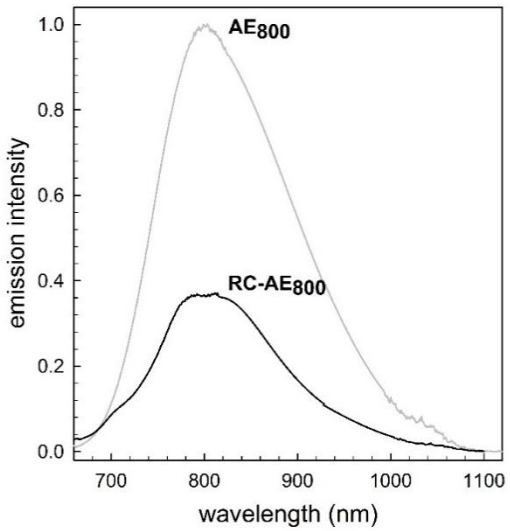

Figure 5. Steady state fluorescence of AE_{800} (grey line) and AE_{800}–RC (black line). Excitation wavelength 650 nm. Conditions: AE (5 μM) in $T_{20}E_1Tx_{0.3}$ and AE–RC (AE/RC 5:1) in $T_{20}E_1Tx_{0.03}$ buffer.

It was shown in our previous work that the presence of the fluorophore AE_{600} in the hybrid system does not affect the photocycle (Figure 6) and, on the contrary, enhances the rate of cytochrome oxidation at the dimer binding site. AE_{800} belongs to the same class of molecules and has comparable size, hence we do not expect any hindrance to electron donation from cytochrome to the reaction center. We settled to test this aspect by looking at the opposite side of the photocycle compared to the investigation reported in our previous paper, *i.e.* the proton uptake that results from the double reduction of the final quinone acceptor to form the quinol. The result of the photocycle is the net reduction of protons in solution and the pH increase associated with the photocycle can be investigated by using a pH-sensitive fluorescent dye, the pyranine, in an unbuffered RC solution.[56]

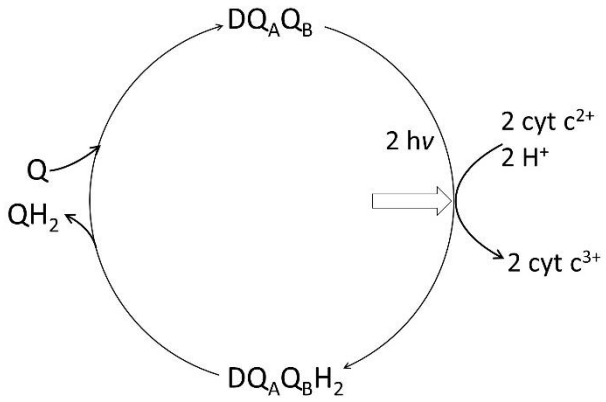

Figure 6. Simplified version of the RC photocycle taking place in presence of exogenous cytochrome and quinone pools and under continuous illumination. The net result is proton sequestration and cytochrome oxidation.

Table 1. Spectroscopic and photophysical data of core moiety and AE_{800}.

Chemical	Solvent	A[a] λ_{max} (nm)	ε[b] ($M^{-1}cm^{-1}$) $\times 10^3$	PL[c] λ_{max} (nm)	Φ_{PL}[d] (%)	τ[e] (ns)	J_{DA}[f] (M^{-1} cm^{-1} nm^4)
Core	$CHCl_3$	570	5.62±0.08	717	23.5	5.96±0.06	n.a.[#]
AE_{800}	$CHCl_3$	635	13.4±0.2	792	7.0	1.20±0.02	n.a.[#]
AE_{800}	$T_{20}E_1TX_3$	650	9.76±0.06	800	5.6	1.22±0.02	$4.77 \cdot 10^{16}$

[a]Absorption maximum, [b]molar extinction coefficient at λ_{max}, [c]emission maximum, [d]absolute photoluminescence quantum yield, [e]excited state lifetime and [f]AE/RC overlap integral reported. [#]Reaction center denaturates in $CHCl_3$

By exciting the pyranine at 450 nm and recording its emission at 510 nm, pH changes associated to the photocycle[56] can be recorded for the RC and the AE_{800}-RC hybrid, as shown in Figure 7. In the presence of exogenous pools of quinone and cytochrome it is possible to drive the photocycle under continuous illumination at 650 nm, the maximum AE_{800} absorption. pH increases as consequence of the proton uptake during the photocycle and the pyranine fluorescence consequently increases. By comparing pH changes obtained in RC and in AE_{800}-RC, the latter results more efficient than the native protein by a factor of 2.2. This experiments confirm that AE_{800} is not detrimental to the photocycle and that the AE_{800}-RC hybrid outperforms the bare protein.

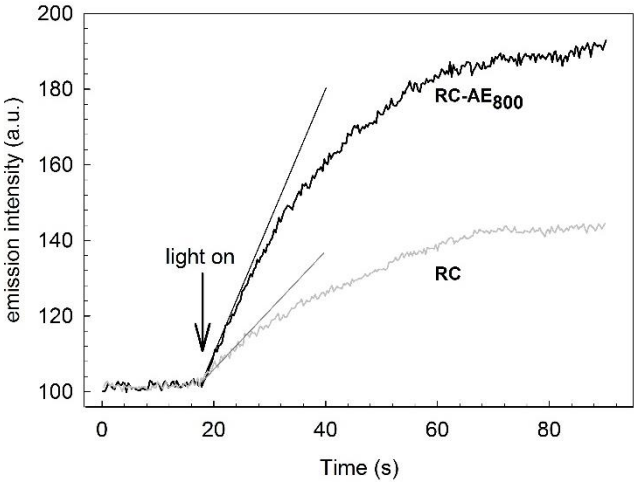

Figure 7. Time course of pyranine fluorescence changes at 510 nm of AE_{800}-RC (black) and RC solution (grey trace) upon excitation at 650 nm. Experimental conditions: 0.5 µM RC, 5 µM cyt c^{2+}, 10 mM ferrocyanide, 100 µM Decylubiquinone, 1 µM pyranine in TX 0.03 w/v, KCl 100 mM. Initial pH adjusted to 6.92. The straight lines represent the initial velocity of the proton uptake and are equal to 3.33±0.05 s^{-1} and 1.34±0.05 s^{-1} in the AE_{800}-RC and RC case, respectively.

Having shown that the RC remains undamaged and fully functional after bioconjugation, attention was turned to the increase of charge-separated state attainable under continuous illumination in AE_{800}-RC as compared to the native protein. Experiments were performed on AE_{800}-RC and pristine RC at 800 nm, where both have the same absorption, and at 450 and 650 nm where the antenna strongly contributes to the absorption of the hybrid systems. Experiments are illustrated in details in the supporting information (see figure S5). The outcome is that AE_{800}-RC outperforms RC by a factor of 5.1 and 2.7 at 450 and 650 nm respectively. The latter value is in good agreement with the increase of 2.4 times in the rate of the AE_{800}-RC photocycle measured by proton uptake at 650 nm. An enhancement factor of 1.7 was also found at 650 nm comparing the hybrid system assembled with a AE_{800}:RC of 2.9±0.1 and the native RC, showing that the higher is the additional cross-section offered by the antenna molecules, the larger is the enhancement effect.

Visible light harvesting antenna effect

Any application of the hybrid systems based on the RC would result very limited if the ability of the bioconjugate system to outperform the reaction center is limited to a single wavelength. This is an important point to address as the use of white light would improve strongly the versatility of such systems. Of course this is not a simple task as the cross-section of the sole protein is already quite high and the additional cross section of the antenna must not be marginal to improve the protein efficiency. It requires careful chiseling in the organic synthesis to fulfil all the spectroscopic requirements, which were not fully attained with other molecules with similar structure.[57] The designed chemical structure successfully fits with this last requirement and irradiation of the AE_{800}-RC hybrid in the interval 350-670 nm showed the ability of AE_{800} to function as white light antenna.

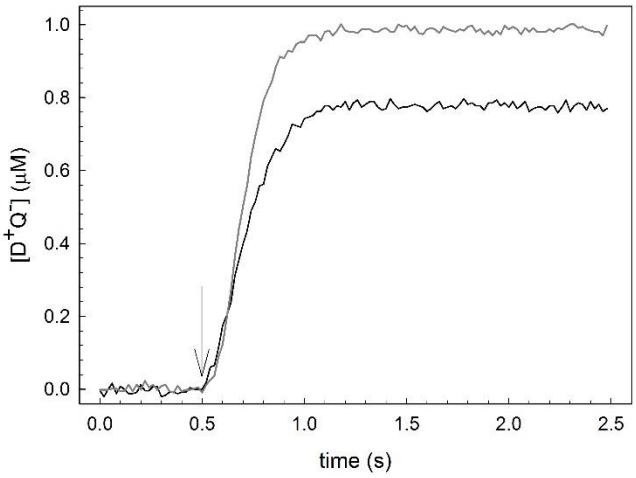

Figure 8. Concentration of charge-separated state $D^+Q_A^-$ generated in AE_{800}-RC (grey line) and native RC (black line) by continuous illumination with a band-pass filter 350-670 nm. Experimental conditions: 1 µM RC, (AE_{800}:RC 4.9±0.1), 100 µM terbutryne in $T_{20}E_1Tx_{0.03}$ buffer with NaCl 150 mM, pH 8.0.

Under sub-saturating white light illumination conditions, the concentration of the charge separated state attained in the hybrid produced a noteworthy 30% increase compared to pristine RC as shown in Figure 8. Once again, this result is due to the spectroscopic characteristics of the artificial antenna that has been designed to absorb in correspondence of low absorption region of the RC, filling the optical gap of the protein by adding only five molecules, and emit in correspondence of a strong absorption of the protein. A similar effect was recently reported for the multiprotein complex PSI bioconjugated with the commercial fluorophore ATTO 590. The authors found the ATTO-PSI complex to be more

efficient than the pristine PSI, although such effect requires a considerable number, in the order of few tens, of dye molecules per protein.[18]

CONCLUSIONS

In this work, a new *ad hoc* designed organic NIR-emitting fluorophore was covalently conjugated with the photosynthetic *R. sphaeroides* RC to produce a hybrid system capable of absorbing light and efficiently extending the absorbance cross section in the broad visible range, also covering regions where RC possesses only weak absorbance.

The recorded data clearly indicate that AE_{800} can efficiently transfer energy to RC enhancing its enzymatic activity without any loss of functional integrity. In fact, at diagnostic wavelengths of 450 nm and 650 nm in AE_{800}-RC the extended absorption cross section generates an almost three-fold improvement versus the native RC, according both to the photocycle and to the charge separation assays.

More interestingly, AE_{800} resulted to remarkably improve the RC photochemical activity also in the broad visible range, producing an increment of charge separated state of 30% in AE_{800}-RC. In conclusion, the AE800-RC complex provides a useful model system for future applications in energy conversion field and paves the way to a new generation of enhanced photosynthetic protein-based hybrid materials.

EXPERIMENTAL SECTION

Synthesis of the organic antenna

Experimental details of all reactions in schemes 1-4 along with full characterization of intermediates and products are presented in the supporting information.

Assembly of the AE_{800}-RC hybrid

The photosynthetic bacterium *Rhodobacter sphaeroides* strain R26 was grown in the Sistrom liquid medium under strictly anoxigenic conditions and under illumination by incandescence 100 W light bulb, as previously published.[58]

Reaction centers were isolated from *R. sphaeroides* R26 following a previously reported procedure[59] and protein purity was checked using the ratio of the absorbance at 280 and 802 nm which was kept below 1.3, and the ratio of the absorbance at 760 and 865 nm kept around 1.

Bioconjugation of AE_{800} was adapted from Milano *et al.*[5] and it was carried out in a solution composed of 25 µM AE_{800} and 2 µM RC in Tris-HCl 20 mM, EDTA 1 mM, Triton X-100 (TX) 0.5% w/v pH 8.0 ($T_{20}E_1TX_{0.5}$). The mixture was incubated for 1 h, loaded on a preconditioned diethylaminoethyl (DEAE)–Sephacel column (DEAE, CAS Number 9013-34-7 from Sigma Aldrich), equilibrated with $T_{20}E_1TX_{0.03}$ and washed with the same buffer to remove the dye excess. The AE_{800}-RC hybrid was finally eluted in a small volume using $T_{20}E_1TX_{0.03}$ added with NaCl 300 mM. The average amount of the dye attached to RC was determined spectrophotometrically at 650 nm. By knowing the extinction coefficient of each component, it is possible to infer the AE_{800}/RC ratio, which is found to slightly vary with preparations. Experiments reported in this manuscript were performed with stock preparations having a ratio AE_{800}/RC = 4.9±0.1. The ratio can be decreased or increased by lowering or increasing the incubation period.

AE_{800}-RC hybrid characterization

Charge separated steady states of RC were obtained by 5 s sample illumination with a 250 W quartz tungsten halogen lamp (QTH), passed through interference filters at 450±10, 650±10 or 800±10 nm. Measurements were conducted at constant photon flux adjusting the lamp irradiance to 10.5 mW/cm^2 at 450 nm, 7.3 mW/cm^2 at 650 nm and 5.9 mW/cm^2 at 800 nm.

The AE_{800} ability of enhancing the RC charge-separated state (CSS) generation in the PAR region was essayed using a QTH lamp filtered by a 350-670 nm band-pass filter and detecting the amount of CSS at 865 nm.

Whenever needed, the Q_B-site functionality was inhibited with terbutryn excess (Chem Service, USA).

Charge recombination kinetics were recorded at 865 nm using a kinetic spectrophotometer of local design implemented with a Hamamatsu R928 photomultiplier and a white-saturating flash used for RC photo-excitation. Data were collected onto a Digital Oscilloscope (Tektronix TDS 3052) and trace deconvolution was performed using a C-code developed in our lab. A detailed description of the apparatus is given elsewhere.[60]

The operational integrity of the RC was checked by recording its photocycle, *i.e.* the entire full enzymatic activity performed by RC under steady-state illumination and in the presence of exogenous electron donors and acceptors. The pH-decrease associated to the photocycle was recorded adapting a previously published protocol.[56] The photocycle was recorded in a solution containing KCl 100 mM, TX 0.03% w/v, cytochrome c^{2+} 5 µM, ferrocyanide 10 mM, decylubiquinone 100 µM, and pyranine (trisodium 8-hydroxypyrene-1,3,6-trisulfonate) 1 µM acting as pH probe. No buffer was added to the solution and the starting pH was set to 7.0 using small amounts of 0.1 M KOH or HCl. The solution was split in two aliquots, one added with AE_{800}-RC and another added with native RC. The final protein concentration was set to 0.5 µM in both aliquots. Samples were carefully kept in dark until starting the experiment and then illuminated with 650 nm filtered light. The changes in the pyranine fluorescence intensity at 510 nm were recorded with a Cary Eclipse (Varian) spectrofluorometer. Pyranine was excited at 450±5 nm. The ability of the excitation light to drive the photocycle was checked and found negligible.

Energy transfer characterization

Steady-state photoluminescence experiments were performed with a FluoroLog (Horiba Jobin-Yvon) spectrofluorometer, using the excitation wavelength of 650±20 nm and emission in the range 680-1100 nm. Time resolved photoluminescence experiments were performed on the AE_{800} with a spectrofluorometer PicoHarp 300 by Time Correlated Single Photon Counting (TSPC). Excitation was provided by a PSL-600 LED and emission was at 750 and 800 nm. Fitting to exponential decay functions was obtained by the deconvolution procedure using a PicoHarp FluoFit software.

The efficiency (E) of Förster energy transfer process (FRET) was calculated from photoluminescence experiments using the following equation:[55]

$$E = 1 - \frac{I_{PL}^{D/A}}{I_{PL}^{D}} \qquad \text{Equation 1}$$

where I_{PL} represents the photoluminescence integral of the energy donor in absence (superscript D) and in presence of the energy acceptor (A) (superscript D/A) respectively. The Förster distance R_0, *i.e.* the distance at which the FRET efficiency is 50%, was estimated with the equation:

$$R_0 = \sqrt[6]{\left(8.79 \times 10^{23} \frac{\text{Å}^6 M}{cm^3}\right)\left(\kappa^2 \cdot \eta^{-4} \cdot \Phi_D \cdot J_{D/A}\right)} \qquad \text{Equation 2}$$

where κ is the dipole orientation factor (taken as $\kappa^2 = 2/3$), η is the refractive index of the medium (η = 1.4 in biological molecules), Φ_D is the fluorescence quantum yield of the energy donor compound and J_{DA} is the overlap integral of the donor emission spectrum with the acceptor absorption.[61]

ASSOCIATED CONTENT

Supporting Information

Data relative to the protein activity and to the characterization of the chemical compounds here presented are supplied as Supporting Information. This material is available free of charge via the Internet at http://pubs.acs.org.

AUTHOR INFORMATION

Corresponding Authors

Massimo Trotta (massimo.trotta@cnr.it) – Istituto per i Processi Chimico Fisici – Consiglio Nazionale delle Ricerche. Via Orabona, 4. 70125 Bari (Italy)

Gianluca Maria Farinola (gianlucamaria.farinola@uniba.it) – Dipartimento di Chimica – Università degli Studi di Bari. Via Orabona, 4. 70125 Bari (Italy).

Present Addresses

[#]Rocco Roberto Tangorra present address: Gruppo Mossi&Ghisolfi – Tortona (AL), Italy.

ACKNOWLEDGMENT

This work was financed by Università degli Studi "Aldo Moro" di Bari (IDEA 2011 project ''BIOEXTEND: Extending enzymatic properties by bioconjugation of enzymes with fluorescent organic oligomers''), PON 02_00563_3316357 Molecular Nanotechnology for Health and Environment MAAT and MIUR-PRIN 2010C4R8M8 (Organizzazione funzionale a livello nanoscopico di (bio)molecole e ibridi per applicazioni nel campo della sensoristica, della medicina e delle biotecnologie). Project n. 31 "PHOEBUS" financed by Regione Puglia.

REFERENCES

(1) Maróti, P., and Trotta, M. (2012) Artificial Photosynthetic Systems, in *CRC Handbook of Organic Photochemistry and Photobiology, Third Edition - Two Volume Set* pp 1289-1324, CRC Press.

(2) Scholes, G. D., Fleming, G. R., Olaya-Castro, A., and van Grondelle, R. (2011) Lessons from nature about solar light harvesting. *Nat Chem 3*, 763-774.

(3) Hohmann-Marriott, M. F., and Blankenship, R. E. (2011) Evolution of Photosynthesis. *Annual Review of Plant Biology 62*, 515-548.

(4) Kamran, M., Friebe, V. M., Delgado, J. D., Aartsma, T. J., Frese, R. N., and Jones, M. R. (2015) Demonstration of asymmetric electron conduction in pseudosymmetrical photosynthetic reaction centre proteins in an electrical circuit. *Nat Commun 6*, 6530.

(5) Milano, F., Tangorra, R. R., Hassan Omar, O., Ragni, R., Operamolla, A., Agostiano, A., Farinola, G. M., and Trotta, M. (2012) Enhancing the Light Harvesting Capability of a Photosynthetic Reaction Center by a Tailored Molecular Fluorophore. *Angewandte Chemie 124*, 11181-11185.

(6) Balzani, V., Credi, A., and Venturi, M. (2008) Photochemical Conversion of Solar Energy. *ChemSusChem 1*, 26-58.

(7) Barber, J. (2007) Biological solar energy. *Philosophical Transactions of the Royal Society A: Mathematical, Physical and Engineering Sciences 365*, 1007-1023.

(8) Swainsbury, D. J., Friebe, V. M., Frese, R. N., and Jones, M. R. (2014) Evaluation of a biohybrid photoelectrochemical cell employing the purple bacterial reaction centre as a biosensor for herbicides. *Biosens Bioelectron 58*, 172-8.

(9) Roth, M., Lewit-Bentley, A., Michel, H., Deisenhofer, J., Huber, R., and Oesterhelt, D. (1989) Detergent structure in crystals of a bacterial photosynthetic reaction centre. *Nature 340*, 659-662.

(10) Operamolla, A., Ragni, R., Milano, F., Roberto Tangorra, R., Antonucci, A., Agostiano, A., Trotta, M., and Farinola, G. (2015) "Garnishing" the photosynthetic bacterial reaction center for bioelectronics. *J Mater Chem C 3*, 6471-6478.

(11) Tangorra, R. R., Operamolla, A., Milano, F., Omar, O. H., Henrard, J., Comparelli, R., Italiano, F., Agostiano, A., De Leo, V., Marotta, R., *et al.* (2015) Assembly of a photosynthetic reaction center with ABA triblock polymersomes: highlights on protein localization. *Photoch Photobio Sci 14*, 1844-1852.

(12) McDermott, G., Prince, S. M., Freer, A. A., Hawthornthwaite-Lawlwss, A. M., Papiz, R. J., Cogdell, R., and Isaacs, N. W. (1995) Crystal structure of an integral membrane light harvesting complex from photosynthetic bacteria. *Nature 374*, 517-521.

(13) R. Roberto Tangorra, A. A., Francesco Milano, Simona la Gatta, Gianluca Farinola, Angela Agostiano, Roberta Ragni, and Massimo Trotta. (2016) Hybrid Interfaces for Electron Transfer and Energy Transfer Based on Photosynthetic Proteins, in *Handbook of Photosynthesis, Third Edition* (Pessarakli, M., Ed.), CRC Press.

(14) Tangorra, R. R., Antonucci, A., Milano, F., la Gatta, S., Operamolla, A., Ragni, R., Agostiano, A., Trotta, M., and Farinola, G. M. (2015) Bio-hybrid photoconverter by covalent functionalization of the photosynthetic reaction center of Rhodobacter sphaeroides with fluorescein isothiocyanate. *MRS Online Proceedings Library 1722*, null-null.

(15) Dutta, P. K., Lin, S., Loskutov, A., Levenberg, S., Jun, D., Saer, R., Beatty, J. T., Liu, Y., Yan, H., and Woodbury, N. W. (2014) Reengineering the optical absorption cross-section of photosynthetic reaction centers. *J Am Chem Soc 136*, 4599-604.

(16) Dutta, P. K., Levenberg, S., Loskutov, A., Jun, D., Saer, R., Beatty, J. T., Lin, S., Liu, Y., Woodbury, N. W., and Yan, H. (2014) A DNA-Directed Light-Harvesting/Reaction Center System. *J Am Chem Soc 136*, 16618-16625.

(17) Yoneda, Y., Noji, T., Katayama, T., Mizutani, N., Komori, D., Nango, M., Miyasaka, H., Itoh, S., Nagasawa, Y., and Dewa, T. (2015) Extension of Light-Harvesting Ability of Photosynthetic Light-Harvesting Complex 2 (LH2) through Ultrafast Energy Transfer from Covalently Attached Artificial Chromophores. *J Am Chem Soc 137*, 13121-13129.

(18) Gordiichuk, P. I., Rimmerman, D., Paul, A., Gautier, D. A., Gruszka, A., Saller, M., de Vries, J. W., Wetzelaer, G. J., Manca, M., Gomulya, W., *et al.* (2016) Filling the Green Gap of a Megadalton Photosystem I Complex by Conjugation of Organic Dyes. *Bioconjug Chem 27*, 36-41.

(19) Mahmoudian, J., Hadavi, R., Jeddi-Tehrani, M., Mahmoudi, A. R., Bayat, A. A., Shaban, E., Vafakhah, M., Darzi, M., Tarahomi, M., and Ghods, R. (2011) Comparison of the Photobleaching and Photostability Traits of Alexa Fluor 568- and Fluorescein Isothiocyanate- conjugated Antibody. *Cell Journal (Yakhteh) 13*, 169-172.

(20) Beverina, L., and Salice, P. (2010) Squaraine Compounds: Tailored Design and Synthesis towards a Variety of Material Science Applications. *Eur J Org Chem*, 1207-1225.

(21) Peng, X., Song, F., Lu, E., Wang, Y., Zhou, W., Fan, J., and Gao, Y. (2005) Heptamethine Cyanine Dyes with a Large Stokes Shift and Strong Fluorescence: A Paradigm for Excited-State Intramolecular Charge Transfer. *J Am Chem Soc 127*, 4170-4171.

(22) Pham, W., Cassell, L., Gillman, A., Koktysh, D., and Gore, J. C. (2008) A near-infrared dye for multichannel imaging. *Chem Commun (Camb)*, 1895-7.

(23) Finikova, O. S., Cheprakov, A. V., Beletskaya, I. P., Carroll, P. J., and Vinogradov, S. A. (2004) Novel versatile synthesis of substituted tetrabenzoporphyrins. *J Org Chem 69*, 522-535.

(24) Bundgaard, E., and Krebs, F. C. (2007) Low band gap polymers for organic photovoltaics. *Sol Energ Mat Sol C 91*, 954-985.

(25) Giancane, G., Ruland, A., Sgobba, V., Manno, D., Serra, A., Farinola, G. M., Omar, O. H., Guldi, D. M., and Valli, L. (2010) Aligning Single-Walled Carbon Nanotubes By Means Of Langmuir-Blodgett Film Deposition: Optical, Morphological, and Photo-electrochemical Studies. *Adv Funct Mater 20*, 2481-2488.

(26) Meier, H. (2005) Conjugated Oligomers with Terminal Donor–Acceptor Substitution. *Angewandte Chemie International Edition 44*, 2482-2506.

(27) Operamolla, A., Colella, S., Musio, R., Loiudice, A., Hassan Omar, O., Melcarne, G., Mazzeo, M., Gigli, G., Farinola, G. M., and Babudri, F. (2011) Low band gap poly(1,4-arylene-2,5-thienylene)s with benzothiadiazole units: Synthesis, characterization and application in polymer solar cells. *Sol Energ Mat Sol C 95*, 3490-3503.

(28) Sgobba, V., Giancane, G., Cannoletta, D., Operamolla, A., Omar, O. H., Farinola, G. M., Guldi, D. M., and Valli, L. (2014) Langmuir-Schaefer films for aligned carbon nanotubes functionalized with a conjugate polymer and photoelectrochemical response enhancement. *ACS applied materials & interfaces 6*, 153-8.

(29) Bolognesi, A., Botta, C., Babudri, F., Farinola, G. M., Hassan, O., and Naso, F. (1999) Silicon-substitued PPV for LED preparation. *Synthetic Met 102*, 919.

(30) Farinola, G. M., and Ragni, R. (2011) Electroluminescent materials for white organic light emitting diodes. *Chem Soc Rev 40*, 3467-3482.

(31) Ragni, R., Operamolla, A., and Farinola, G. M. (2013) Synthesis of electroluminescent conjugated polymers for OLEDs, in *Organic Light-Emitting Diodes* (Buckley, A., Ed.) pp 3-48.

(32) Ellinger, S., Graham, K. R., Shi, P., Farley, R. T., Steckler, T. T., Brookins, R. N., Taranekar, P., Mei, J., Padilha, L. A., Ensley, T. R., *et al.* (2011) Donor–Acceptor–Donor-based π-Conjugated Oligomers for Nonlinear Optics and Near-IR Emission. *Chemistry of Materials 23*, 3805-3817.

(33) Kitamura, C., Tanaka, S., and Yamashita, Y. (1996) Design of Narrow-Bandgap Polymers. Syntheses and Properties of Monomers and Polymers Containing Aromatic-Donor and o-Quinoid-Acceptor Units. *Chemistry of Materials 8*, 570-578.

(34) Yang, Y., Farley, R. T., Steckler, T. T., Eom, S.-H., Reynolds, J. R., Schanze, K. S., and Xue, J. (2008) Near infrared organic light-emitting devices based on donor-acceptor-donor oligomers. *Appl Phys Lett 93*, 163305.

(35) Yang, Y., Farley, R. T., Steckler, T. T., Eom, S.-H., Reynolds, J. R., Schanze, K. S., and Xue, J. (2009) Efficient near-infrared organic light-emitting devices based on low-gap fluorescent oligomers. *J Appl Phys 106*, 044509.

(36) Bunz, U. H. F. (2000) Poly(aryleneethynylene)s: Syntheses, Properties, Structures, and Applications. *Chemical Reviews 100*, 1605-1644.

(37) Bunz, U. H. F. (2005) Synthesis and Structure of PAEs. *Advanced Polymer Science 177*, 1-52.

(38) Operamolla, A., Ragni, R., Omar, O. H., Iacobellis, G., Cardone, A., Babudri, F., and Farinola, G. M. (2012) *Curr. Org. Synth. in press*.

(39) Pescitelli, G., Omar, O. H., Operamolla, A., Farinola, G. M., and Di Bari, L. (2012) Chiroptical Properties of Glucose-Substituted Poly(p-phenylene-ethynylene)s in Solution and Aggregate State. *Macromolecules 45*, 9626-9630.

(40) Blakskjaer, P., and Gothelf, K. V. (2006) Synthesis of an elongated linear oligo(phenylene ethynylene)-based building block for application in DNA-programmed assembly. *Org Biomol Chem 4*, 3442-3447.

(41) Hu, W., Zhu, N., Tang, W., and Zhao, D. (2008) Oligo(p-phenyleneethynylene)s with Hydrogen-Bonded Coplanar Conformation. *Org Lett 10*, 2669-2672.

(42) Yin, C., Hong, B., Gong, Z., Zhao, H., Hu, W., Lu, X., Li, J., Li, X., Yang, Z., Fan, Q., *et al.* (2015) Fluorescent oligo(p-phenyleneethynylene) contained amphiphiles-encapsulated magnetic nanoparticles for targeted magnetic resonance and two-photon optical imaging in vitro and in vivo. *Nanoscale 7*, 8907-19.

(43) Cai, T., Zhou, Y., Wang, E., Hellström, S., Zhang, F., Xu, S., Inganäs, O., and Andersson, M. R. (2010) Low bandgap polymers synthesized by FeCl3 oxidative polymerization. *Sol Energ Mat Sol C 94*, 1275-1281.

(44) Wang, E., Hou, L., Wang, Z., Hellström, S., Mammo, W., Zhang, F., Inganäs, O., and Andersson, M. R. (2010) Small Band Gap Polymers Synthesized via a Modified Nitration of 4,7-Dibromo-2,1,3-benzothiadiazole. *Org Lett 12*, 4470-4473.

(45) Uno, T., Takagi, K., and Tomoeda, M. (1980) Synthesis of Bisfurazanobenzo-2, 1, 3-thiadiazole and Related Compounds. *Chem Pharm Bull 28*, 1909-1912.

(46) Zoombelt, A. P., Fonrodona, M., Wienk, M. M., Sieval, A. B., Hummelen, J. C., and Janssen, R. A. J. (2009) Photovoltaic Performance of an Ultrasmall Band Gap Polymer. *Org Lett 11*, 903-906.

(47) Mohanakrishnan, A. K., Hucke, A., Lyon, M. A., Lakshmikantham, M. V., and Cava, M. P. (1999) Functionalization of 3,4-ethylenedioxythiophene. *Tetrahedron 55*, 11745-11754.

(48) Bolognesi, A., DiGianvincenzo, P., Giovanella, U., Mendichi, R., and Schieroni, A. G. (2008) Polystyrene functionalized with EDOT oligomers. *European Polymer Journal 44*, 793-800.

(49) Lo, S.-C., Harding, R. E., Brightman, E., Burn, P. L., and Samuel, I. D. W. (2009) The development of phenylethylene dendrons for blue phosphorescent emitters. *J Mater Chem 19*, 3213-3227.

(50) Xiang, W., Gupta, A., Kashif, M. K., Duffy, N., Bilic, A., Evans, R. A., Spiccia, L., and Bach, U. (2013) Cyanomethylbenzoic acid: an acceptor for donor-pi-acceptor chromophores used in dye-sensitized solar cells. *ChemSusChem 6*, 256-60.

(51) Siebrand, W. (1967) Radiationless Transitions in Polyatomic Molecules. I. Calculation of Franck—Condon Factors. *The Journal of Chemical Physics 46*, 440.

(52) Feher, G. (1971) Some chemical and physical properties of a bacterial reaction center particle and its primary photochemical reactants. *Photochem Photobiol 14*, 373-87.

(53) Ragni, R., Omar, O. H., Tangorra, R. R., Milano, F., Vona, D., Operamolla, A., La Gatta, S., Agostiano, A., Trotta, M., and Farinola, G. M. (2014) Bursting photosynthesis: designing ad-hoc fluorophores to complement the light harvesting capability of the photosynthetic reaction center. *MRS Online Proceedings Library 1689*.

(54) Belviso, B. D., Tangorra, R. R., Milano, F., Hassan Omar, O., la Gatta, S., Ragni, R., Agostiano, A., Farinola, G. M., Caliandro, R., and Trotta, M. (2016) Crystallographic analysis of the photosynthetic reaction center from Rhodobacter sphaeroides bioconjugated with an artificial antenna. *MRS Advances FirstView*, 1-12.

(55) Lakowicz, J. R. (2006) *Principles of Fluorescence Spectroscopy*, 3rd edition ed., Springer, New York.

(56) Agostiano, A., Mavelli, F., Milano, F., Giotta, L., Trotta, M., Nagy, L., and Maroti, P. (2004) pH-sensitive fluorescent dye as probe for proton uptake in photosynthetic reaction centers. *Bioelectrochemistry 63*, 125-8.

(57) la Gatta, S., Hassan Omar, O., Agostiano, A., Milano, F., Tangorra, R. R., Operamolla, A., Chiorboli, C., Argazzi, R., Natali, M., Trotta, M., *et al.* (2015) A far-red emitting aryleneethynylene fluorophore used as light harvesting antenna in hybrid assembly with the photosynthetic reaction center. *MRS Advances*, 1-6.

(58) Italiano, F., Rinalducci, S., Agostiano, A., Zolla, L., De Leo, F., Ceci, L. R., and Trotta, M. (2012) Changes in morphology, cell wall composition and soluble proteome in Rhodobacter sphaeroides cells exposed to chromate. *Biometals 25*, 939-949.

(59) Milano, F., Italiano, F., Agostiano, A., and Trotta, M. (2009) Characterisation of RC-proteoliposomes at different RC/lipid ratios. *Photosynth Res 100*, 107-12.

(60) Milano, F., Agostiano, A., Mavelli, F., and Trotta, M. (2003) Kinetics of the quinone binding reaction at the Q(B) site of reaction centers from the purple bacteria Rhodobacter sphaeroides reconstituted in liposomes. *Eur J Biochem 270*, 4595-4605.

(61) Hink, M., Visser, N., Borst, J., van Hoek, A., and Visser, A. W. G. (2003) Practical Use of Corrected Fluorescence Excitation and Emission Spectra of Fluorescent Proteins in Förster Resonance Energy Transfer (FRET) Studies. *J Fluoresc 13*, 185-188.

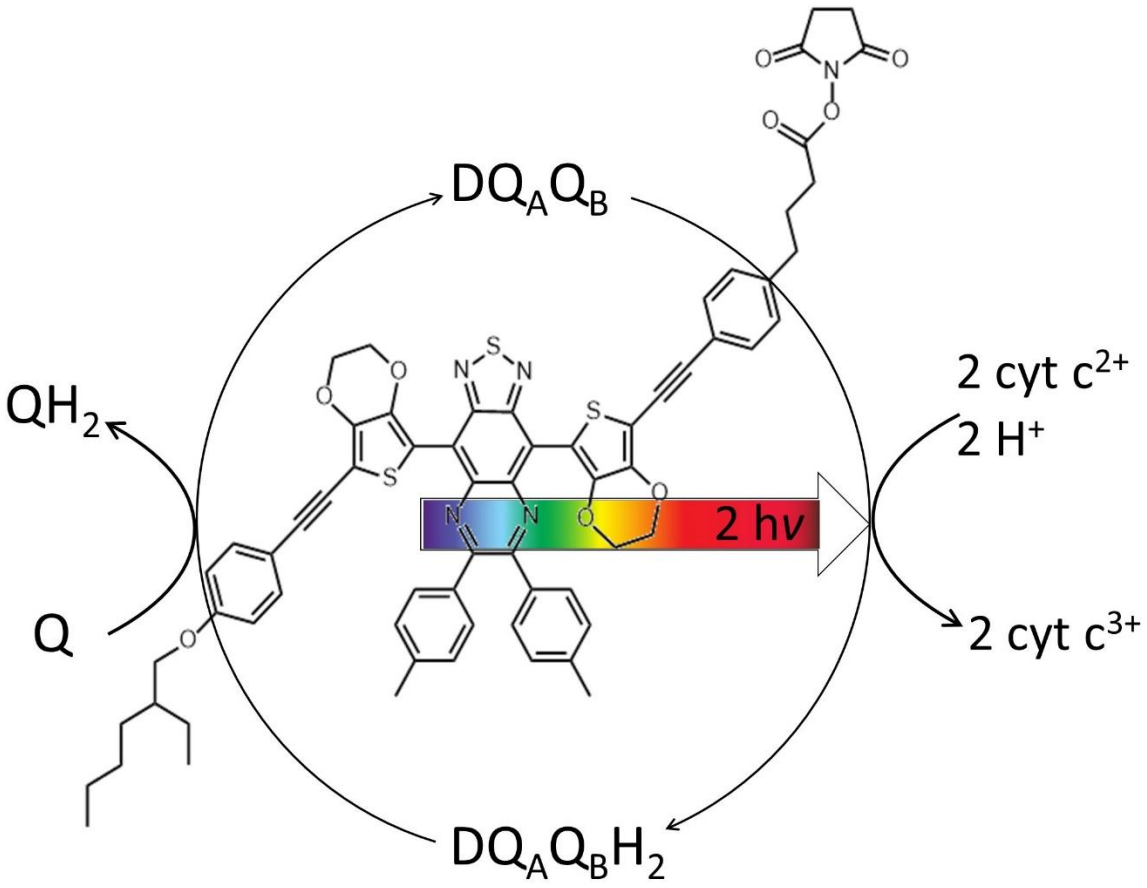
DQAQB
QH2
Q
2 cyt c2+
2 H+
2 cyt c3+
2 hν
DQAQBH2